K. Tulasidevi, A. Hemashekar / International Journal of Engineering Research and Applications (IJERA) ISSN: 2248-9622 www.ijera.com
Vol. 2, Issue4, July-August 2012, pp.1738-1744

Analysis And Control Of A Doubly Fed Induction Generator Under Unbalanced Voltage Sags

K. Tulasidevi,
II year M.tech
PG student
SVPCET,PUTTUR,

A. Hemashekar,
M.tech.,(ph.D)
Associate professor, HOD,
SVPCET,PUTTUR,

Abstract

This paper deals with the control of doubly fed induction generators to ride through unbalanced voltage sags. A control strategy is proposed by choosing certain current reference values in the positive and negative sequences so that the torque and the dc voltage are kept detailing the control scheme of each converter while considering the effect of the crowbar protection. The control strategy is validated by means of simulation.

I. INTRODUCTION

WIND power is one of the most promising renewable energy sources after the progress undergone during the last decades. However, its integration into power systems has a number of technical challenges concerning security of supply, in terms of reliability, availability, and power quality. Many relevant contributions have been recently done to face such challenges, ranging from the control of active [1] and reactive [2] power, to the modeling [3], [4] of different classes of wind turbines Such oscillations are provoked by the negative sequence components injected by the unbalanced disturbance.

This paper has been organized as follows. In Section II, the control scheme under balanced conditions is discussed. The unbalanced case is analyzed in Section III. The proposed technique is validated by means of simulations in Section IV. The obtained results are discussed in Section V, and finally, the conclusions are summarized in Section VI.

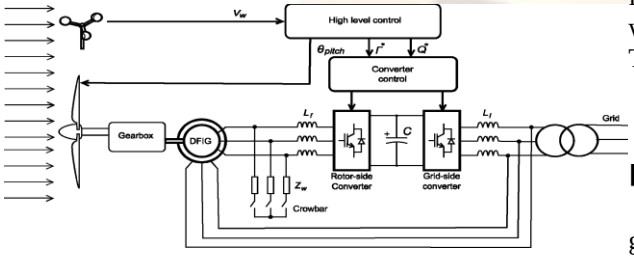

Fig.1. General System scheme

II. CONTROL SCHEME UNDER BALANCED CONDITIONS

The general scheme under analysis can be seen in Fig. 1. The DFIG is attached to the wind turbine by means of a gearbox. The DFIG stator windings are connected directly to the grid while the rotor windings are connected to a back-to-back converter (see Fig. 2). The converter is composed of the grid side converter connected to the grid and the rotor-side converter connected to the wound rotor windings. The converter set points are established by the so-called high-level controller. It uses the knowledge of the wind speed and the grid active and reactive power requirements to determine the optimum turbine pitch angle and the torque and reactive power set points referenced to the converter.

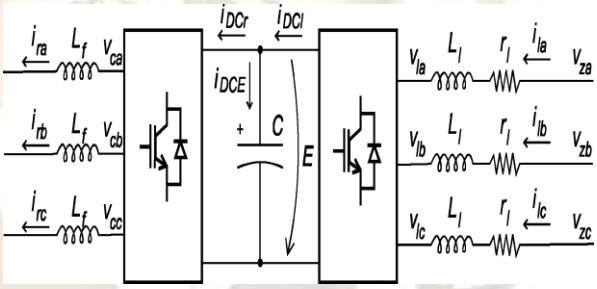

Fig. 2. Back-Back converter

A. Grid-Side Converter

In the grid-side converter, the dc bus voltage and reactive power references determine the current references, which determine the voltages to be applied in the grid side.

1) System Equations: In a synchronous reference frame, the grid-side voltage equations can be written as

The dc bus voltage can be expressed as

$$\begin{Bmatrix} v_{zq} \\ v_{zd} \end{Bmatrix} - \begin{Bmatrix} v_{lq} \\ v_{ld} \end{Bmatrix} = \begin{bmatrix} R_l & -L_l\omega_c \\ L_l\omega_c & R_l \end{bmatrix} \begin{Bmatrix} i_{lq} \\ i_{ld} \end{Bmatrix} + \begin{bmatrix} L_l & 0 \\ 0 & L_l \end{bmatrix} \frac{d}{dt} \begin{Bmatrix} i_{lq} \\ i_{ld} \end{Bmatrix}. \quad (1)$$

Active and reactive power provided by the grid-side converter can be written as $Pz = 3/2(vzq\ ilq + vzdild)$ and $Qz = 3/2(vzq\ ild - vzdilq)$.

The dc bus voltage can be expressed as

$$E = E_0 + \frac{1}{C}\int_0^t (i_{DCl} - i_{DCr})\,dt. \quad (2)$$

2) **Reference Quantities:** The grid-side converter controls the reactive power and dc bus voltage. The *q*-axismay be aligned to the grid voltage allowing active and reactive decoupled control. To control the reactive power, a *ild* reference is computed as

$$i_{ld}^{*} = \frac{2Q_z^{*}}{3v_{zq}}. \qquad (3)$$

The active power, which is responsible for the evolution of the dc bus voltage is controlled by the *ilq* component. A linear controller is usually designed to control the dc bus voltage.

*3***) Current Loops Implementation:** The current control is
done by the following state linearization feedback [18]:

$$\begin{Bmatrix} v_{lq} \\ v_{ld} \end{Bmatrix} = \begin{Bmatrix} -\hat{v}_{lq} + v_{zq} - L_l\omega_e i_{ld} \\ -\hat{v}_{ld} + L_l\omega_e i_{lq} \end{Bmatrix} \qquad (4)$$

where the ˆ*vlq* and ˆ*vld* are the output voltages of the current
controller. The decoupling leads to

$$\frac{d}{dt}\begin{Bmatrix} i_{lq} \\ i_{ld} \end{Bmatrix} = \begin{bmatrix} -\frac{R_l}{L_l} & 0 \\ 0 & -\frac{R_l}{L_l} \end{bmatrix}\begin{Bmatrix} i_{lq} \\ i_{ld} \end{Bmatrix} + \begin{bmatrix} \frac{1}{L_l} & 0 \\ 0 & \frac{1}{L_l} \end{bmatrix}\begin{Bmatrix} \hat{v}_{lq} \\ \hat{v}_{qd} \end{Bmatrix}. \qquad (5)$$

B. **Rotor-Side Converter**

In the rotor-side converter, the referenced torque and reactive power determine the current references, which determine the voltages to be applied in the rotor side.

1) Machine Equations: It is usually assumed that when the Stator and rotor windings are placed sinusoid ally and symmetrically, the magnetically saturation effects and the capacitance of all the windings are negligible. The relation between voltages and currents on a synchronous reference *qd* can be written as

$$\begin{Bmatrix} v_{sq} \\ v_{sd} \\ v_{rq} \\ v_{rd} \end{Bmatrix} = \begin{bmatrix} L_s & 0 & M & 0 \\ 0 & L_s & 0 & M \\ M & 0 & L_r & 0 \\ 0 & M & 0 & L_r \end{bmatrix}\frac{d}{dt}\begin{Bmatrix} i_{sq} \\ i_{sd} \\ i_{rq} \\ i_{rd} \end{Bmatrix} + \begin{bmatrix} R_s & L_s\omega_c & 0 & M\omega_c \\ -L_s\omega_c & R_s & -M\omega_c & 0 \\ 0 & sM\omega_c & R_r & sL_r\omega_c \\ -sM\omega_c & 0 & -sL_r\omega_c & R_r \end{bmatrix}\begin{Bmatrix} i_{sq} \\ i_{sd} \\ i_{rq} \\ i_{rd} \end{Bmatrix} \qquad (6)$$

Linkage fluxes can be written as

$$\begin{Bmatrix} \lambda_{sq} \\ \lambda_{sd} \\ \lambda_{rq} \\ \lambda_{rd} \end{Bmatrix} = \begin{bmatrix} L_s & 0 & M & 0 \\ 0 & L_s & 0 & M \\ M & 0 & L_r & 0 \\ 0 & M & 0 & L_r \end{bmatrix}\begin{Bmatrix} i_{sq} \\ i_{sd} \\ i_{rq} \\ i_{rd} \end{Bmatrix}. \qquad (7)$$

The torque can expressed as

$$\Gamma_m = \frac{3}{2}PM\,(i_{sq}i_{rd} - i_{sd}i_{rq}). \qquad (8)$$

The reactive power yields

$$Q_s = \frac{3}{2}\left(v_{sq}i_{sd} - v_{sd}i_{sq}\right). \qquad (9)$$

2) Reference Quantities*:* Orientating the synchronous reference *qd* with the stator flux vector so that *λsd* = 0, the rotor current references can be computed as

$$\begin{Bmatrix} i_{rq}^{*} \\ i_{rd}^{*} \end{Bmatrix} = \begin{Bmatrix} \frac{\frac{2}{3}L_s Q_s^{*} + M v_{sq} i_{rd} + v_{sd}\lambda_{sq}}{M v_{sd}} \\ \frac{2L_s\Gamma_m^{*}}{3PM\lambda_{sq}} \end{Bmatrix}. \qquad (10)$$

3) Current Loops Implementation: The control of the current is done by linearizing the current dynamics using the following state feedback.

$$\begin{Bmatrix} v_{rq} \\ v_{rd} \end{Bmatrix} = \begin{Bmatrix} \hat{v}_{rq} + M\left(\omega_e - \omega_r\right)i_{sd} + L_r\left(\omega_e - \omega_r\right)i_{rd} \\ \hat{v}_{rd} - M\left(\omega_e - \omega_r\right)i_{sq} - L_r\left(\omega_e - \omega_r\right)i_{rq}. \end{Bmatrix} \qquad (11)$$

By neglecting stator current transients, the decoupling leads to

$$\frac{d}{dt}\begin{Bmatrix} i_{rq} \\ i_{rd} \end{Bmatrix} = -\begin{bmatrix} \frac{R_r}{L_r} & 0 \\ 0 & \frac{R_r}{L_r} \end{bmatrix}\begin{Bmatrix} i_{rq} \\ i_{rd} \end{Bmatrix} + \begin{bmatrix} \frac{1}{L_r} & 0 \\ 0 & \frac{1}{L_r} \end{bmatrix}\begin{Bmatrix} \hat{v}_{rq} \\ \hat{v}_{rd} \end{Bmatrix}. \qquad (12)$$

C. Current Controllers Tuning

Controllers have been designed using the so-called internal mode control (IMC) methodology. The parameters of a PI controller to obtain a desired time constant *τ* are obtained as

$$K_p = \frac{L}{\tau}, \qquad K_i = \frac{R}{\tau}. \qquad (13)$$

The currents and voltages have been limited according to the converter operating limits. PI controllers have been designed with anti wind up in order to prevent control instabilities when the controllers exceed the limit values.

D. Crowbar Protection

The so-called crowbar is connected to avoid over voltages in the dc bus due to excessive power flowing from the rotor inverter to the grid-side converter, guaranteeing ride through operation of the generator when voltage sags or other disturbances occur. The crowbar is triggered when the dc voltage reaches a threshold *v*crow−*c* and disconnects when it goes below another threshold *v*crow−*d*.

III. CONTROL SCHEME UNDER UNBALANCED CONDITIONS

In this section, nonsymmetrical voltage sags are considered. Such unbalanced sags imply negative sequence components in all the relevant quantities. This section analyzes a whole back-to-back converter taking into account both the positive and negative sequence components, and proposes a technique to control optimally both the dc bus voltage and the torque when unbalanced voltage sags occur.

As far as unbalanced systems are concerned, it is useful to express three-phase quantities *xabc* = *{xa, xb, xc}T* in direct
and inverse components as

$$\mathbf{x} = e^{j\omega_e t + j\theta_0}\mathbf{x}^p + e^{-j\omega_e t - j\theta_0}\mathbf{x}^n \quad (14)$$

where $\mathbf{x} = 2/3\,(x_a + ax_b + a^2 x_c)$, $a = e^{j2\pi/3}$, $\mathbf{x}^p = x_d^p + jx_q^p$, and $\mathbf{x}^n = x_d^n + jx_q^n$. In this section, voltages, currents, and fluxes are regarded as a composition of such positive and negative sequences.

A. Grid-Side Converter Analysis

1) Voltage Equations: Considering two rotating reference frames at $+\omega e$ and $-\omega e$, the voltage equations for the positive and negative sequences yield

$$\mathbf{v}_{zqd}^p - \mathbf{v}_{lqd}^p = (R_l + j\omega_e L_l)\,\mathbf{i}_{lqd}^p + L_l \frac{d\mathbf{i}_{lqd}^p}{dt} \quad (15)$$

$$\mathbf{v}_{zqd}^n - \mathbf{v}_{lqd}^n = (R_l - j\omega_e L_l)\,\mathbf{i}_{lqd}^n + L_l \frac{d\mathbf{i}_{lqd}^n}{dt} \quad (16)$$

2) Active and Reactive Power: Active and reactive power can be written as [13]

$$P_l = \frac{3}{2}\left[P_{l0} + P_{l\cos}\cos(2\omega_e t) + P_{l\sin}\sin(2\omega_e t)\right] \quad (17)$$

$$Q_l = \frac{3}{2}\left[Q_{l0} + Q_{l\cos}\cos(2\omega_e t) + Q_{l\sin}\sin(2\omega_e t)\right] \quad (18)$$

Where

$$\begin{Bmatrix} P_{l0} \\ P_{l\cos} \\ P_{l\sin} \\ Q_{l0} \\ Q_{l\cos} \\ Q_{l\sin} \end{Bmatrix} = \begin{bmatrix} v_{zd}^p & v_{zq}^p & v_{zd}^n & v_{zq}^n \\ v_{zd}^n & v_{zq}^n & v_{zd}^p & v_{zq}^p \\ v_{zq}^n & -v_{zd}^n & -v_{zq}^p & v_{zd}^p \\ v_{zq}^p & -v_{zd}^p & v_{zq}^n & -v_{zd}^n \\ v_{zq}^n & -v_{zd}^n & v_{zq}^p & -v_{zd}^p \\ -v_{zd}^n & -v_{zq}^n & v_{zd}^p & v_{zq}^p \end{bmatrix} \begin{Bmatrix} i_{ld}^p \\ i_{lq}^p \\ i_{ld}^n \\ i_{lq}^n \end{Bmatrix}. \quad (19)$$

It can be noted that both active and reactive power have three different components each, and hence with the four regulatable currents *ipld* , *iplq* , *inld* , and *inlq* , only four of such six powers can be controlled.

B. Machine-Side Converter Analysis

1) **Voltage Equations:** Considering two rotating reference frames at $+\omega e$ and $-\omega e$, the voltage equations for the positive and negative sequences can be obtained as

$$\begin{Bmatrix} \mathbf{v}_s^p \\ \mathbf{v}_r^p \end{Bmatrix} = \begin{bmatrix} L_s & M \\ M & L_r \end{bmatrix} \frac{d}{dt} \begin{Bmatrix} \mathbf{i}_s^p \\ \mathbf{i}_r^p \end{Bmatrix} + \begin{bmatrix} R_s + jL_s\omega_e & jM\omega_e \\ jM(\omega_e - \omega_r) & R_r + jL_r(\omega_e - \omega_r) \end{bmatrix} \begin{Bmatrix} \mathbf{i}_s^p \\ \mathbf{i}_r^p \end{Bmatrix} \quad (20)$$

$$\begin{Bmatrix} \mathbf{v}_s^n \\ \mathbf{v}_r^n \end{Bmatrix} = \begin{bmatrix} L_s & M \\ M & L_r \end{bmatrix} \frac{d}{dt} \begin{Bmatrix} \mathbf{i}_s^n \\ \mathbf{i}_r^n \end{Bmatrix} + \begin{bmatrix} R_s - j\omega_e L_s & -j\omega_e M \\ +jM(-\omega_e - \omega_r) & R_r + jL_r(-\omega_e - \omega_r) \end{bmatrix} \times \begin{Bmatrix} \mathbf{i}_s^n \\ \mathbf{i}_r^n \end{Bmatrix}. \quad (21)$$

2) Stator Power Expression: The apparent stator power can be expressed as

$$\mathbf{S}_s = P_s + jQ_s = \frac{3}{2}\mathbf{v}_s \mathbf{i}_s^*. \quad (22)$$

Using (14), we have

$$\mathbf{S}_s = (e^{j\omega_e t + j\theta_0}\mathbf{v}_s^p + e^{-j\omega_e t - j\theta_0}\mathbf{v}_s^n) \times \left((e^{j\omega_e t + j\theta_0})^* \mathbf{i}_s^{p*} + (e^{-j\omega_e t - j\theta_0})^* \mathbf{i}_s^{n*}\right) \quad (23)$$

$$\mathbf{S}_s = \mathbf{v}_s^p \mathbf{i}_s^{p*} + \mathbf{v}_s^n \mathbf{i}_s^{n*} + e^{j2\omega_e t + j2\theta_0}\mathbf{v}_s^p \mathbf{i}_s^{n*} + e^{-j2\omega_e t - j2\theta_0}\mathbf{v}_s^n \mathbf{i}_s^{p*}. \quad (24)$$

Taking into account $\mathbf{x}_s^i = x_{sd}^i + jx_{sq}^i$, and rearranging it gives $\mathbf{S}_s = P_s + jQ_s$, with

$$P_s = \frac{3}{2}\left[P_{s0} + P_{s\cos}\cos(2\omega_e t + 2\theta_0) + P_{s\sin}\sin(2\omega_e t + 2\theta_0)\right] \quad (25)$$

$$Q_s = \frac{3}{2}\left[Q_{s0} + Q_{s\cos}\cos(2\omega_e t + 2\theta_0) + Q_{s\sin}\sin(2\omega_e t + 2\theta_0)\right] \quad (26)$$

where

$$\begin{Bmatrix} P_{s0} \\ P_{s\cos} \\ P_{s\sin} \\ Q_{s0} \\ Q_{s\cos} \\ Q_{s\sin} \end{Bmatrix} = \begin{bmatrix} v_{sd}^p & v_{sq}^p & v_{sd}^n & v_{sq}^n \\ v_{sd}^n & v_{sq}^n & v_{sd}^p & v_{sq}^p \\ v_{sq}^n & -v_{sd}^n & -v_{sq}^p & v_{sd}^p \\ v_{sq}^p & -v_{sd}^p & v_{sq}^n & -v_{sd}^n \\ v_{sq}^n & -v_{sd}^n & v_{sq}^p & -v_{sd}^p \\ -v_{sd}^n & -v_{sq}^n & v_{sd}^p & v_{sq}^p \end{bmatrix} \begin{Bmatrix} i_{sd}^p \\ i_{sq}^p \\ i_{sd}^n \\ i_{sq}^n \end{Bmatrix}. \quad (27)$$

Substituting stator currents in (27)

$$\begin{Bmatrix} P_{s0} \\ P_{s\cos} \\ P_{s\sin} \\ Q_{s0} \\ Q_{s\cos} \\ Q_{s\sin} \end{Bmatrix} = \frac{1}{L_s} \begin{bmatrix} v_{sd}^p & v_{sq}^p & v_{sd}^n & v_{sq}^n \\ v_{sd}^n & v_{sq}^n & v_{sd}^p & v_{sq}^p \\ v_{sq}^n & -v_{sd}^n & -v_{sq}^p & v_{sd}^p \\ v_{sq}^p & -v_{sd}^p & v_{sq}^n & -v_{sd}^n \\ v_{sq}^n & -v_{sd}^n & v_{sq}^p & -v_{sd}^p \\ -v_{sd}^n & -v_{sq}^n & v_{sd}^p & v_{sq}^p \end{bmatrix} \times \begin{Bmatrix} \lambda_{sd}^p - Mi_{rd}^p \\ \lambda_{sq}^p - Mi_{rq}^p \\ \lambda_{sd}^n - Mi_{rd}^n \\ \lambda_{sq}^n - Mi_{rq}^n \end{Bmatrix} \quad (28)$$

3) Rotor Power Expression: The apparent rotor power can be expressed as

$$\mathbf{S}_r = P_r + jQ_r = \frac{3}{2}\mathbf{v}_r \mathbf{i}_r^* \quad (29)$$

$$\mathbf{S}_r = \frac{3}{2}\left(e^{j(\omega_e - \omega_r)t + j\theta_{r0}}\mathbf{v}_r^p + e^{-j(\omega_e + \omega_r)t - j\theta_{r0}}\mathbf{v}_r^n\right) \times \left(e^{j(\omega_e - \omega_r)t + j\theta_{r0}}\mathbf{i}_r^p + e^{-j(\omega_e + \omega_r)t - j\theta_{r0}}\mathbf{i}_r^n\right)^*. \quad (30)$$

Using (14), we have

$$\mathbf{S}_r = \frac{3}{2}\left[\mathbf{v}_r^p \mathbf{i}_r^{p*} + \mathbf{v}_r^n \mathbf{i}_r^{n*} + e^{j2\omega_e t + 2j\theta_{r0}}\mathbf{v}_r^p \mathbf{i}_r^{n*} + e^{j-2\omega_e t - j2\theta_{r0}}\mathbf{v}_r^n \mathbf{i}_r^{p*}\right]. \quad (31)$$

Taking into account $\mathbf{x}_s^i = x_{sd}^i + jx_{sq}^i$, and rearranging and analyzing the active rotor power

$$P_r = \frac{3}{2}\left[P_{r0} + P_{r\cos}\cos(2\omega_e t + 2\theta_{r0}) + P_{r\sin}\sin(2\omega_e t + 2\theta_{r0})\right] \quad (32)$$

where

$$\begin{Bmatrix} P_{r0} \\ P_{r\cos} \\ P_{r\sin} \end{Bmatrix} = \begin{bmatrix} v_{cd}^p & v_{cq}^p & v_{cd}^n & v_{cq}^n \\ v_{cd}^n & v_{cq}^n & v_{cd}^p & v_{cq}^p \\ v_{cq}^n & -v_{cd}^n & -v_{cq}^p & v_{cd}^p \end{bmatrix} \begin{Bmatrix} i_{rd}^p \\ i_{rq}^p \\ i_{rd}^n \\ i_{rq}^n \end{Bmatrix}. \quad (33)$$

4) Torque Expression: Analogously, electrical torque can be expressed as

$$\Gamma = \frac{P}{2}\frac{3}{2}\left[\Gamma_0 + \Gamma_{\sin}\sin(2\omega_e t) + \Gamma_{\cos}\cos(2\omega_e t)\right] \quad (34)$$

where

$$\begin{Bmatrix} \Gamma_0 \\ \Gamma_{\cos} \\ \Gamma_{\sin} \end{Bmatrix} = \frac{M}{L_s} \begin{bmatrix} -\lambda_{sq}^p & \lambda_{sd}^p & -\lambda_{sq}^n & \lambda_{sd}^n \\ \lambda_{sd}^n & \lambda_{sq}^n & -\lambda_{sd}^p & -\lambda_{sq}^p \\ -\lambda_{sq}^n & \lambda_{sd}^n & -\lambda_{sq}^p & \lambda_{sd}^p \end{bmatrix} \begin{Bmatrix} i_{rd}^p \\ i_{rq}^p \\ i_{rd}^n \\ i_{rq}^n \end{Bmatrix}. \quad (35)$$

C. Reference Current Calculation

Since there are eight degrees of freedom (the rotor-side currents *iprd*, *iprq* , *inrd*, and *inrq* , and the grid-side currents *ipld* , *iplq* ,*inld* , and *inlq*), eight control objectives may be chosen. This implies that it is not possible to eliminate all the oscillations provoked by the unbalance. In this paper, the main objective is to ride through voltage dips. To this end, it has been chosen to determine the currents to keep certain values of T^*_0, $T^*_{\cos}$, $T^*_{\sin}$, and Q^*_{s0} for the rotor-side converter and $P*l0$, $P*l\cos$, $P*l\sin$

.

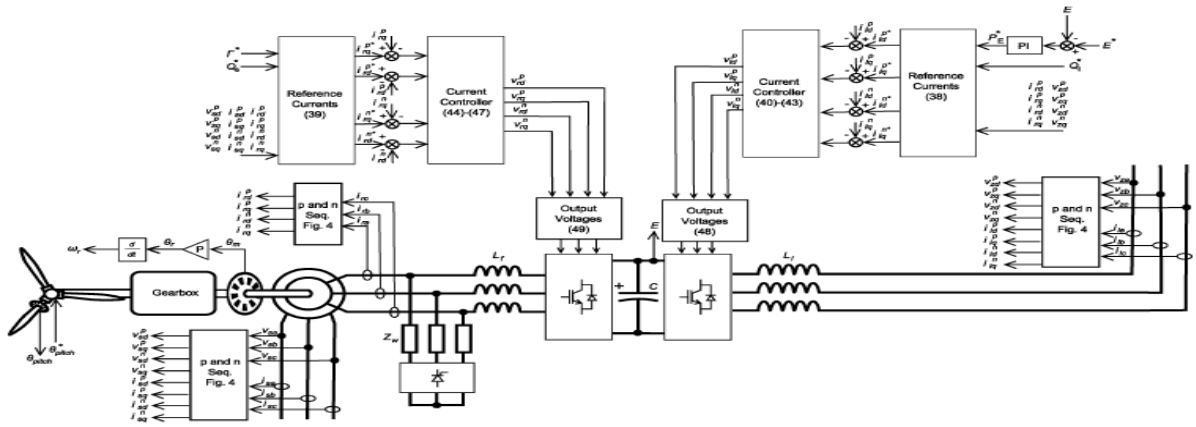

Fig.3. General Control Scheme

*Pr*0 can be regarded as the average power delivered, while *P*rcos and *P*rsin are the rotor power oscillating terms. Such terms will cause dc voltage oscillations, and hence they can be canceled by choosing

$$P^*_{l\cos} = P_{r\cos} \quad P^*_{l\sin} = P_{r\sin}. \tag{36}$$

*Pl*0 can be computed as

$$P^*_{l0} = P_{r0} + P^*_E \tag{37}$$

where $P*E$ is the output of the dc voltage linear controller.

The grid reference currents can be computed from (19), (33),
(36), and (37) as

$$\begin{Bmatrix} i^{p*}_{ld} \\ i^{p*}_{lq} \\ i^{n*}_{ld} \\ i^{n*}_{lq} \end{Bmatrix} = \begin{bmatrix} v^p_{zd} & v^p_{zq} & v^n_{zd} & v^n_{zq} \\ v^n_{zd} & v^n_{zq} & v^p_{zd} & v^p_{zq} \\ v^n_{zq} & -v^n_{zd} & -v^p_{zq} & v^p_{zd} \\ v^p_{zq} & -v^p_{zd} & v^n_{zq} & -v^n_{zd} \end{bmatrix}^{-1} \left(\begin{Bmatrix} P_E \\ 0 \\ 0 \\ Q^*_{l0} \end{Bmatrix} + \begin{bmatrix} v^p_{cd} & v^p_{cq} & v^n_{cd} & v^n_{cq} \\ v^n_{cd} & v^n_{cq} & v^p_{cd} & v^p_{cq} \\ v^n_{cq} & -v^n_{cd} & -v^p_{cq} & v^p_{cd} \\ 0 & 0 & 0 & 0 \end{bmatrix} \begin{Bmatrix} i^p_{rd} \\ i^p_{rq} \\ i^n_{rd} \\ i^n_{rq} \end{Bmatrix} \right). \tag{38}$$

The rotor reference currents can be computed from (28) and
(35) as

$$\begin{Bmatrix} i^{p*}_{rd} \\ i^{p*}_{rq} \\ i^{n*}_{rd} \\ i^{n*}_{rq} \end{Bmatrix} = \begin{bmatrix} -\lambda^p_{sq} & \lambda^p_{sd} & -\lambda^n_{sq} & \lambda^n_{sd} \\ \lambda^n_{sd} & \lambda^n_{sq} & -\lambda^p_{sd} & -\lambda^p_{sq} \\ -\lambda^n_{sq} & \lambda^n_{sd} & -\lambda^p_{sq} & \lambda^p_{sd} \\ -v^p_{sq} & v^p_{sd} & -v^n_{sq} & v^n_{sd} \end{bmatrix}^{-1} \begin{Bmatrix} \frac{2}{P}\frac{2}{3}\frac{L_s}{M}\Gamma^*_0 \\ \frac{2}{P}\frac{2}{3}\frac{L_s}{M}\Gamma^*_{\cos} \\ \frac{2}{P}\frac{2}{3}\frac{L_s}{M}\Gamma^*_{\sin} \\ \frac{1}{M}\left[L_s Q^*_{s0} - \lambda^p_{sd}v^p_{sq} + \lambda^p_{sq}v^p_{sd} - \lambda^n_{sd}v^n_{sq} + \lambda^n_{sq}v^n_{sd}\right] \end{Bmatrix}. \tag{39}$$

D. Control Implementation

1) Positive and Negative Components Calculation: The positive and negative sequence components calculation is done by using the Clarke transformation, rotating either *ejωe t* or *e−jωe t, and* finally, applying a notch-filter at 2*ωe* to eliminate the opposite sequence. The technique is exemplified in Fig. 4. For the rotor voltages and currents, the rotation applied is either *ej* (*ωe* −*ωr*)*t* or *ej* (−*ωe* −*ωr*)*t* .

*2***) Reference Orientation***:* The rotating references have been aligned with the stator voltage so that *vpsq* = 0. Nevertheless, *vpsq* has not been substituted in previous expressions for the sake of describing general results. Orientation may be done computing the required *θ*0 assuming a constant *ωe* or using a PLL [21] to determine both *ωe* and *θ*0.

*E***. Controllers Linearization and Tuning**

a) Grid-Side: Similarly to the balanced case developed in
Section II-A3, the control of the current is done by linearizing the current dynamics using

$$\hat{\mathbf{v}}^p_{zqd} = \mathbf{v}^p_{zqd} - \mathbf{v}^p_{lqd} - j\omega_e L_l \mathbf{i}^p_{lqd} \tag{40}$$

$$\hat{\mathbf{v}}^n_{zqd} = \mathbf{v}^n_{zqd} - \mathbf{v}^n_{lqd} + j\omega_e L_l \mathbf{i}^n_{lqd}. \tag{41}$$

Since there are eight degrees of freedom (the rotor-side currents *iprd*, *iprq* , *inrd*, and *inrq* , and the grid-side currents *ipld* , *iplq* ,*inld* , and *inlq*), eight control objectives may be chosen. This implies that it is not possible to eliminate all the oscillations provoked by the unbalance. In this paper, the main objective is to ride through voltage dips. Hence, it is important to keep the torque and dc bus voltage as

constant as possible and to keep reasonable values of reactive power. It can be noted that $P*l0$, $P*l\cos$, and $P*l\sin$ are directly linked to the dc bus voltage. The dc voltage E is regulated by means of a linear controller whose output is the power demanded by the grid-side converter. Considering the power terms $Pr0$, $Pr\cos$, and $Pr\sin$ in the rotor side converter, $Pr0$ can be regarded as the average power delivered, while $Pr\cos$ and $Pr\sin$ are the rotor power oscillating terms. Such terms will cause dc voltage oscillations, and hence they Can be canceled by choosing

The decoupled system yields

$$\frac{d\mathbf{i}_{lqd}^{p}}{dt} = \frac{\hat{\mathbf{v}}_{zqd}^{p} - R_l \mathbf{i}_{lqd}^{p}}{L_l} \quad (42)$$

$$\frac{d\mathbf{i}_{lqd}^{n}}{dt} = \frac{\hat{\mathbf{v}}_{zqd}^{n} - R_l \mathbf{i}_{lqd}^{n}}{L_l}. \quad (43)$$

b) Rotor-Side: Analogously to Section II-B3

$$\hat{\mathbf{v}}_r^p = \mathbf{v}_r^p - jM(\omega_e - \omega_r)\mathbf{i}_s^p - jL_r(\omega_e - \omega_r)\mathbf{i}_r^p \quad (44)$$

$$\hat{\mathbf{v}}_r^n = \mathbf{v}_r^n - jM(-\omega_e - \omega_r)\mathbf{i}_s^n - jL_r(-\omega_e - \omega_r)\mathbf{i}_r^n. \quad (45)$$

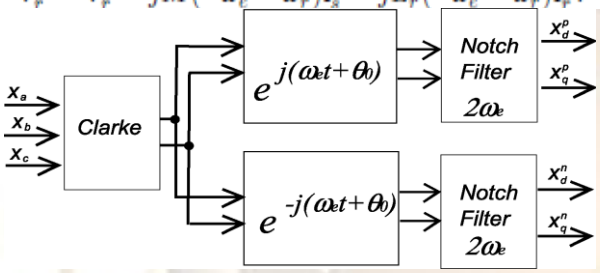

Fig. 4. Positive and negative components calculation.

$$\frac{d\mathbf{i}_r^p}{dt} = \frac{\hat{\mathbf{v}}_r^p - R_r \mathbf{i}_r^p}{L_r} \quad (46)$$

$$\frac{d\mathbf{i}_r^n}{dt} = \frac{\hat{\mathbf{v}}_r^n - R_r \mathbf{i}_r^n}{L_r}. \quad (47)$$

c) Controller Tuning: The controllers can be designed using classical linear control techniques. As in Section II-C, a PI controller is used, tuned according to IMC [19]. For a time constant τ , the parameters obtained yield $Kp = L\,\tau$ and $Ki = R\tau$.

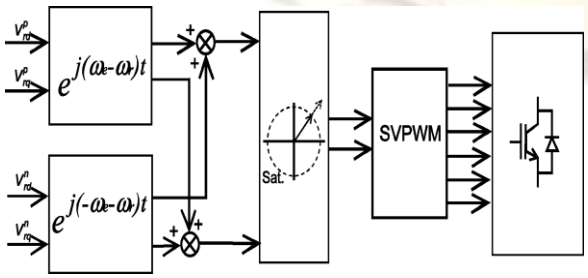

Fig. 5. Output voltage calculation: rotor-side converter example.

F. Output Voltage Calculation

The output voltages calculation is done by summing the resulting positive and negative sequence voltages in the stationary reference frame. For the line side

$$\mathbf{v}_l = e^{j\omega_e t}\mathbf{v}_l^p + e^{-j\omega_e t}\mathbf{v}_l^n. \quad (48)$$

For the rotor side

$$\mathbf{v}_r = e^{j(\omega_e - \omega_r)t}\mathbf{v}_r^p + e^{j(-\omega_e - \omega_r)t}\mathbf{v}_r^n. \quad (49)$$

The resulting voltages are limited according to the converter rating. The final voltages can be applied using standard space vector pulse width modulation (SVPWM) techniques. The tsechnique is exemplified for the rotor-side converter case in Fig. 5.

IV. SIMULATION RESULTS

In order to evaluate the ride-through capability of the proposed scheme, the system has been simulated with severe voltage sags, making the control work at the maximum output voltage and dealing with the triggering of the crowbar protection. The data of the simulated system may be seen in Table I.

In order to compare the presented control scheme and some existing techniques, the following three cases have been studied.

T1 Balanced control case: It is the classical control approach, which does not take into account the possibility of unbalanced voltage disturbances. It is described I number of references [5]–[11]. In this case, the synchronous reference frame is aligned with the stator flux and the control is implemented, as described in Section II.

T2 Unbalanced control 1: The technique described in Section III is applied, with the exception that it does not use the rotor power compensation.

T3 Unbalanced control 2: The technique described in Section III is applied, also considering the rotor power compensation.

It is known that such torque sign changes can provoke serious damage to the turbine mechanics. For the technique T3, the torque remains stable close to −4000 N-·m. Furthermore, the speed is clearly more stable for the T3 case, as illustrated in Fig. 7.Regarding dc voltage bus evolution, it is shown in Fig. 8(a) that the proposed technique T3 shows important advantages over technique T2, which does not compensate the rotor power. The dc voltage oscillation for T1 is of 106 V while for T3 is 21 V, meaning an oscillation reduction of more than 80%.

.

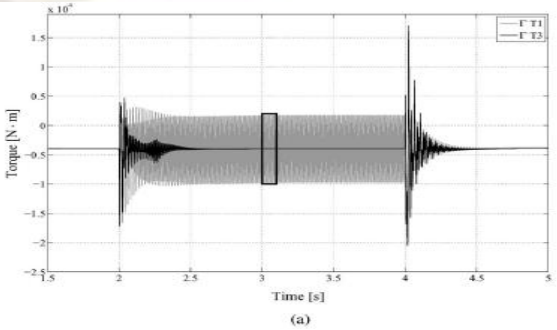

(a)

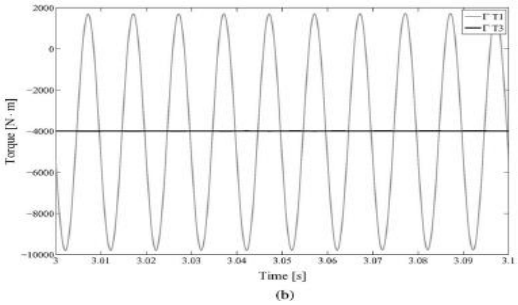

Fig. 6. Torque response comparison of a two-phase voltage sag of 50% using the standard control technique T1 without considering unbalanced conditions and the technique T3 proposed in this paper. (a) Torque response for the whole voltage sag time. (b) Torque evolution in the center of the sag.

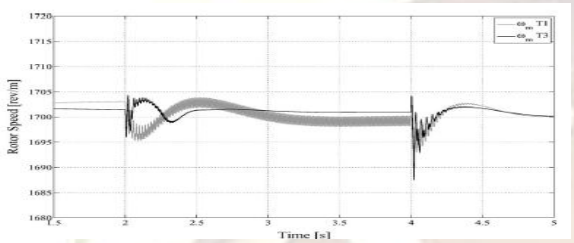

Fig. 7. Rotor speed comparison of a two-phase voltage sag of 50% using the standard control technique T1 without considering unbalanced conditions and the technique T3 proposed in this paper.

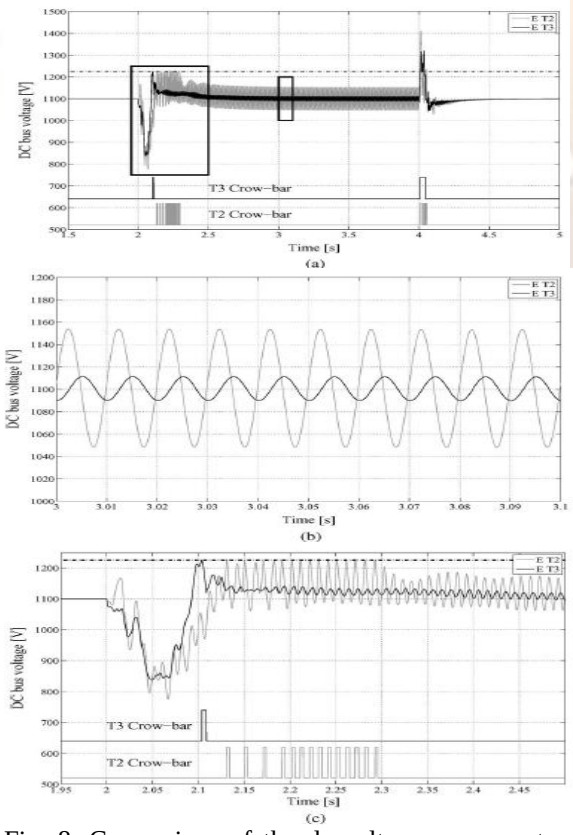

Fig. 8. Comparison of the dc voltage response to a 50% two-phase voltage-sag using T3 or T2. (a) DC voltage response for the whole voltage sag time. (b) DC voltage evolution in the center of the sag. (c) DC voltage response in the initial time of the sag.

The evolution of different voltages for the technique T3 during the sag are shown in Fig. 9. It can be noted that the grid voltage unbalance suffered as a consequence of the two-phase sag is compensated by also applying unbalanced voltages both to the rotor- and grid-side converters..

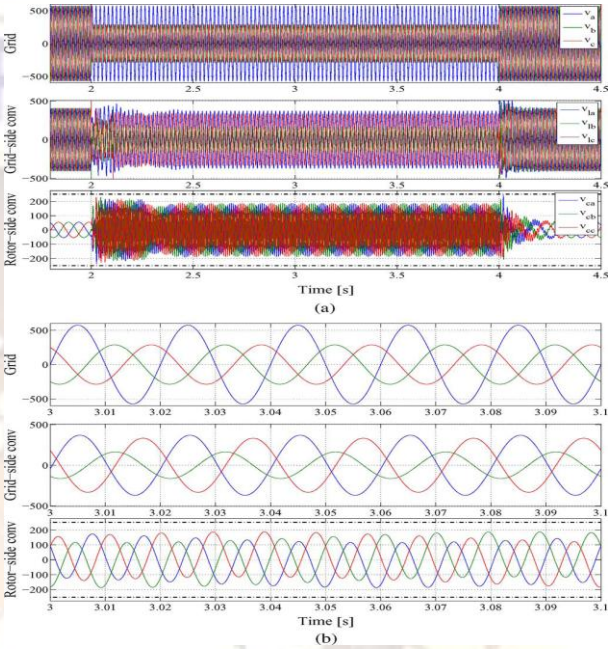

Fig. 9. Voltage response to a two-phase voltage sags of 50 %. (a) Voltages
evolution for the whole voltage sag time. (b) Voltages evolution in the center of the sag.

V. RESULTS AND IMPLEMENTATION DISCUSSION

The technique T3 has proven to provide the most optimum results. Such results are achieved by implementing eight current control loops, whose reference values are computed as described in (38) and (39). The increased complexity of the control scheme in comparison with classical "balanced" control techniques allow to have more degrees of freedom in the control and to apply unbalanced voltage both in the DFIG rotor and the grid-side converters.

Concerning the obtained results, the most relevant observed improvements can be summarized as

1) An optimum torque control is achieved. After a transient,
the desired torque is obtained. This is remarkable in comparison to the behavior of the "balanced" technique T1,
where the torque has important oscillations that may result

in serious damage to the mechanics of the wind turbine.

2) The dc voltage oscillations are minimized as shown in Fig. 8. This is obtained by compensating the rotor power transients in the dc bus voltage control. Instability of the dc voltage may lead to repetitive limit cycles, where the crowbar is permanently connecting and disconnecting.

3) Under balanced operation, the system operates equally to the "balanced" techniques, not introducing any unbalance in the power grid.. The DSP has to develop the following tasks in each switching cycle:

1) Performing of the analog to digital conversion of the measured voltages and currents shown in Fig. 3.

2) Acquisition of the position from an encoder or resolver signal and computation of the rotor speed.

3) Determination of the grid electrical angle and pulsation either assuming that the frequency is fixed and known or using a phase-locked loop (PLL) to determine both angle and frequency.

4) Computation of the *qd* components in the positive and negative sequences, according to Fig.4. The notch filters may be implemented using Butterworth digital filters.

5) Execution of the PI current loops and computation of the output voltage taking into account the feed forward decoupling terms.

VI. CONCLUSION

This paper has presented a control technique to deal with DFIG operation under unbalanced voltage sags, taking into account the presence of positive and negative sequence components in voltages and currents. Both rotor- and grid-side converters are considered, which detail the control scheme to be used in each converter while considering the effect of the crowbar protection. The proposed technique achieves an almost constant torque during the unbalanced sag and compensates the rotor. power oscillations by ssdefining appropriate grid-side converter reference currents so that the dc voltage is kept stable. The control strategy has been validated by means of simulations.

REFERENCES

[1] C. Luo, H. Banakar, S. Baike, and O. Boon-Teck, "Strategies to smooth wind power fluctuations of wind turbine generator," *IEEE Trans. Energy Convers.*, vol. 22, no. 2, pp. 341–349, Jun. 2007.

[2] M.Kayikci and J. Milanovic, "Reactive power control strategies for DFIG based plants," *IEEE Trans. Energy Convers.*, vol. 22, no. 2, pp. 389–396, Jun. 2007.

[3] C. Eisenhut, F. Krug, C. Schram, and B. Klockl, "Wind-turbine model for system simulations near cut-in wind speed," *IEEE Trans. Energy Convers.*, vol. 22, no. 2, pp. 414–420, Jun. 2007.

[4] K. Seul-Ki and K. Eung-Sang, "PSCAD/EMTDC-based modeling and analysis of a gearless variable speed wind turbine," *IEEE Trans. Energy Convers.*, vol. 22, no. 2, pp. 421–430, Jun. 2007.

[5] R. Pena, J. J. C. Clare, and G. Asher, "Doubly fed induction generator using back-to-back PWM converters and its application to variable-speed wind-energy generation," *Proc. Inst. Elect. Eng. Electric Power Appl.*, vol. 143, no. 3, pp. 231–241, 1996.

[6] P. Ledesma and J. Usaola, "Doubly fed induction generator model for transient stability analysis," *IEEE Trans. Energy Convers.*, vol. 20, no. 2, pp. 388–397, Jun. 2005.

[7] Y. Lei, A. Mullane, G. Lightbody, and R. Yacamini, "Modeling of the wind turbine with a doubly fed induction generator for grid integration studies," *IEEE Trans. Energy Convers.*, vol. 21, no. 1, pp. 257–264, Mar. 2006